

Universal Behavior of Linear Alkanes in a Confined Medium: Toward a Calibrationless Use of Thermoporometry

Naïma Bahloul,^{†,‡} Mohamed Baba,[‡] and Jean-Marie Nedelec^{*,†}

Laboratoire des Matériaux Inorganiques, UMR CNRS 6002, and Laboratoire de Photochimie Moléculaire et Macromoléculaire, UMR CNRS 6505, Ecole Nationale Supérieure de Chimie de Clermont Ferrand et Université Blaise Pascal, 24 Avenue des Landais, 63174 Aubière Cedex, France

Received: May 31, 2005; In Final Form: July 21, 2005

A general law has been derived for predicting the transition temperature of linear alkanes confined in nanoporous materials from the simple knowledge of the free solvent transition temperature. This law is in very good agreement with the one previously determined for substituted benzenes, attesting a possible universal behavior of confined solvents.

The lowering of the transition temperature of liquids confined in porous materials was first observed a very long time ago. By the end of the 19th century, the theoretical thermodynamical description of this phenomenon was given.¹ In particular, the transition temperature shift, ΔT , is related to the size of the pore in which the solvent is confined. In the late 1970s, it was proposed to use this observation as a tool to study the texture of divided materials.² In principle, the recording of the differential scanning calorimetry (DSC) curve of a given solvent confined in a porous material would allow one to determine its pore size distribution. The main limitation in applying this technique known as thermoporometry is the lack of knowledge of the $R_p(1/\Delta T)$ law for a given solvent. Another required law is the evolution of the apparent energy of crystallization, W_a , as a function of ΔT . Several authors have been using thermoporometry to study the texture of porous materials of polymers, but in fact, until very recently, the studies were mainly limited to a few solvents including water and benzene.^{3–7} Thanks to the use of porous materials of known texture (measured by gas sorption, for instance), calibrations have been proposed for various solvents including cyclohexane,⁸ acetonitrile,⁹ carbon tetrachloride,¹⁰ and substituted benzenes.¹¹ At this step, thermoporometry can be used as a substitution tool for gas sorption measurements¹² as can the related NMR cryoporometry.¹³ We have shown recently^{14,15} that thermoporometry can also be used very efficiently to characterize soft matter like polymers or gels. In the case of polymers, an analogy is proposed between the meshes constituting the polymer network and the pores of a solid material. When the polymer is swollen in a solvent, the latter experiences a shift of its transition temperature, as observed in porous media. The application of thermoporometry can give access to the size distribution of the meshes and thus a direct image of the reticulation of the network. This is very crucial information in particular if one wants to

study the photoaging behavior of the polymer. Of course, in this case, the choice of the solvent is very important, and this motivated our systematic search for calibration procedures. The aim of this paper is to report original results concerning the possibility to extrapolate calibration curves for any solvent belonging to a specific family. Results concerning substituted benzenes have been published recently,¹¹ and this paper will focus on linear alkanes. We will show that it is possible to derive a general law that relates T_p , the crystallization temperature of a given alkane confined in a pore of radius R_p , to the normal transition temperature of the solvent, T_0 .

Nanoporous silica gels A–E were used as standard materials for calibration. They were prepared by controlled hydrolysis/condensation of tetraethoxysilane ($\text{Si}(\text{OC}_2\text{H}_5)_4$) following procedures described elsewhere.¹⁶ The materials used in this study are the same as those reported in previous work.^{8,11,14,17} Textural data of the reference samples are displayed in Table 1.

Linear alkane $\text{C}_n\text{H}_{2n+2}$ ($n = 6, 7, 10, 12$, and 18) solvents of HPLC grade were used without further purification. The first four solvents were calibrated following the procedure described in ref 11, and the last one ($n = 18$) was used as a control solvent.

As an illustration, thermograms recorded for n -hexane confined in the reference porous silica gels are displayed in Figure 1a. The endothermic peak corresponds to the melting of the free solvent and has been used for the determination of T_0 . Calibration curves are displayed in parts b and c of Figure 1 for the $R_p(1/\Delta T)$ and $W_a(\Delta T)$ curves, respectively. As already performed in our previous work, fitting equations of the following form were considered:

$$R_p = t \exp\left(\frac{-1}{c\Delta T}\right) \quad (1)$$

$$W_a = W_0 \exp\left(\frac{\Delta T}{f}\right) \quad (2)$$

where R_p is the pore radius, $\Delta T = T_p - T_0$ is the freezing point depression, with T_0 corresponding to the onset of the endotherm of the melting of the pure solvent (see Figure 1), T_p is the

* Corresponding author. E-mail: j-marie.nedelec@univ-bpclermont.fr. Phone: 00 33 (0)473407105. Fax: 00 33 (0)473407108.

[†] Laboratoire des Matériaux Inorganiques, UMR CNRS 6002.

[‡] Laboratoire de Photochimie Moléculaire et Macromoléculaire, UMR CNRS 6505.

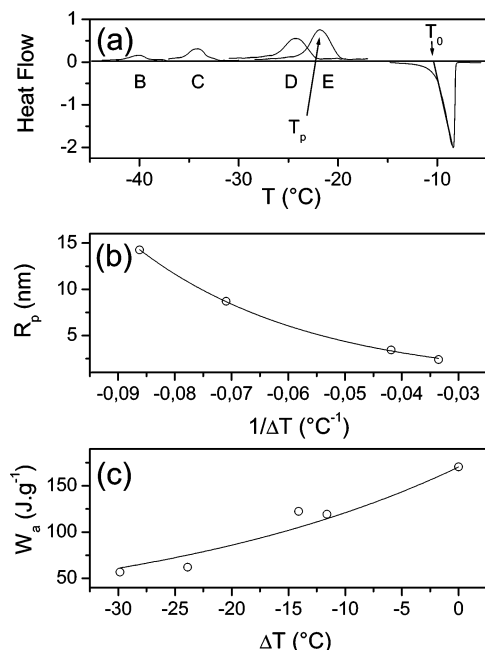


Figure 1. Calibration curves for *n*-hexane: DSC thermograms (a); $R_p(1/\Delta T)$ curve (b); $W_a(\Delta T)$ curve (c). The lines in parts b and c are the best exponential fits.

TABLE 1: Textural Data and Corresponding Standard Deviations of the Nanoporous Silica Gels

| sample | SSA ($\text{m}^2\cdot\text{g}^{-1}$) | σ ($\text{m}^2\cdot\text{g}^{-1}$) | V_p ($\text{cm}^3\cdot\text{g}^{-1}$) | σ ($\text{cm}^3\cdot\text{g}^{-1}$) | R_p (nm) | σ (nm) |
|--------|---|--|--|---|---------------|------------------|
| A | 537 | 12.8 | 0.333 | 0.001 | 1.75 | 0.05 |
| B | 532 | 9.5 | 0.696 | 0.028 | 2.40 | 0.30 |
| C | 472.7 | 1.5 | 0.922 | 0.082 | 3.42 | 0.67 |
| D | 166.2 | 3.2 | 0.991 | 0.071 | 8.70 | 1.24 |
| E | 183.1 | 1 | 1.327 | 0.072 | 14.25 | 1.41 |

crystallization temperature for the confined solvent (T_p is measured at the peak maximum of the crystallization of the confined solvent), t is the thickness of the layer of solvent remaining adsorbed on the surface of the pore and which does not take part in the crystallization, W_0 is the enthalpy of crystallization of the free solvent, and c and f are two constants depending on the solvent.

Table 2 gives the parameters t , c , W_0 , and f determined from curve fitting of experimental results for $n = 6, 7, 10$, and 12 .

Figure 2 shows the plot of T_p (freezing temperature in the pore with radius R_p) versus T_0 (normal freezing temperature of the bulk solvent) for the four linear alkanes that have been calibrated and for octadecane.

For each silica sample, a linear relationship, $T_p = aT_0 + b$, with an excellent correlation coefficient, is found. The slopes, a , of these straight lines are practically equal to the unit (average value $a = 1.04$) as observed for substituted benzene solvents,¹¹ and no significant dependence on the sample radii is pointed out. On the other hand, the origin ordinates, b , depend on the mean pore size of the gels according to the following expression:

$$b = \frac{-125.12}{R_p} \quad (3)$$

The global expression consequently becomes

$$T_p = 1.04T_0 - (125.12/R_p) \quad (4)$$

with T_p and T_0 in kelvins and R_p in nanometers.

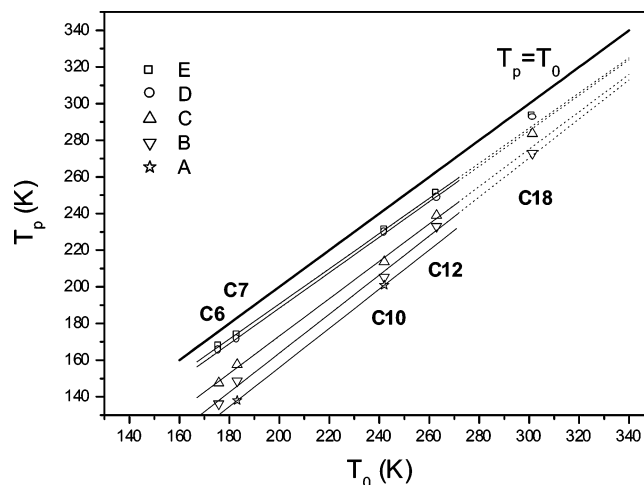


Figure 2. Evolution of T_p as a function of T_0 for various linear alkanes ($n = 6, 7, 10, 12$, and 18) confined in nanoporous silica gels A (☆), B (▽), C (Δ), D (○), and E (□). The continuous lines correspond to the $n = 6, 7, 10$, and 12 best linear fit. The dotted lines represent an extension of the fit to the $n = 18$ alkane. The bold line corresponds to the $T_p = T_0$ line which would correspond to an infinite pore size.

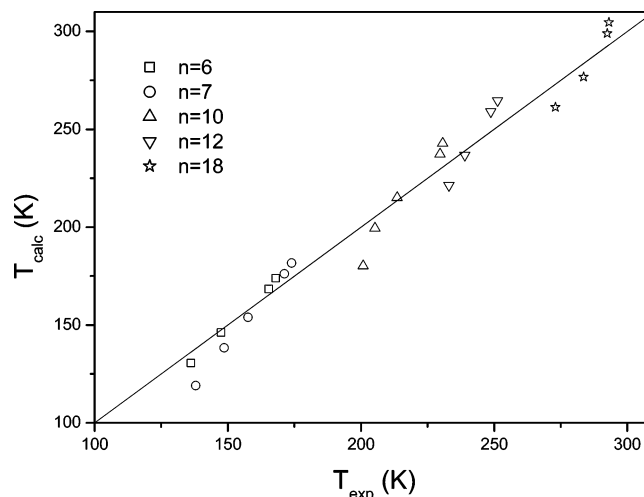


Figure 3. Plot of T_{calcd} calculated with eq 4 as a function of T_{exptl} measured for the various nanoporous gels and the different solvents. The $y = x$ line is drawn as a guide, and all points are well distributed along this line.

TABLE 2: Curve Fitting Parameters for $R_p(1/\Delta T)$ and $W_a(\Delta T)$ for Various Linear Alkanes ($n = 6, 7, 10$, and 12)

| n in $\text{C}_n\text{H}_{2n+2}$ | t (nm) | c | W_0 ($\text{J}\cdot\text{cm}^{-3}$) | f |
|------------------------------------|----------|-------|---|--------|
| 6 | 1.85 | 0.063 | 88.98 | -36.04 |
| 7 | 1.35 | 0.060 | 100.19 | -33.43 |
| 10 | 0.94 | 0.033 | 229.40 | -14.75 |
| 12 | 0.85 | 0.030 | 170.42 | -29.23 |

Experimental points of $\text{C}_{18}\text{H}_{38}$ are nicely predicted by the model. This is clear evidence of a possible extrapolation of thermoporosimetry data for unknown solvents by the simple knowledge of their melting temperature, T_0 . The validity of the derived expression is a priori restricted to similar solvents, in this case linear alkanes. It is quite striking to note that the a value seems to be independent of the family of solvents, since the same value (1.02) was found for aromatic solvents. Figure 3 finally presents the correlation between the T_p values determined by eq 4 and the experimental values for the five linear alkanes where the straight line corresponds to the $T_{\text{calcd}} = T_{\text{exptl}}$ curve. As can be seen, the predictive quality of the model is fairly good.

Equation 4 can be related to the Kelvin relation:

$$\Delta T = \frac{2v_l\gamma_{ls}T_0}{\Delta H_0 R_p} \quad (5)$$

where γ_{ls} , v_l , and ΔH_0 are the liquid–solid interfacial tension, liquid phase molar volume, and molar heat of liquid–solid transition, respectively. These parameters are considered constant in Kelvin's equation, whereas they obviously vary with temperature. This is a strong limitation in the predictive application of Kelvin's equation. In our approach, this problem is circumvented, since we determine W_a , the apparent energy of crystallization, and also its variation with temperature. This procedure is possible thanks to the use of calibration samples of known texture (in particular, total porous volume).

If we consider however Kelvin's equation, our experimental results seem to suggest that the $2v_l\gamma_{ls}T_0/\Delta H_0$ factor is equal to $-125.12 \text{ K}\cdot\text{nm}$ and is independent of the length of the alkane chain. The liquid phase molar volume, T_0 , and ΔH_0 increase when the length of the alkane chain, n , increases. Because of the strong structural similitude between the linear alkane, γ_{ls} is nearly constant. For instance, γ_{ls} is equal to 0.0285 and 0.0277 kg/s^2 for $\text{C}_{10}\text{H}_{22}$ and $\text{C}_{18}\text{H}_{38}$, respectively. All of these parameters vary both with the nature of the solvent and with temperature. Our experimental results indicate that all evolutions compensate each other to yield a global constant factor equal to $-125.12 \text{ K}\cdot\text{nm}$ for the linear alkanes. The same observation was done in the case of substituted benzenes but with of course a distinct value. The knowledge of this value would be enough, in principle, to predict the behavior of any solvent belonging to a specific chemical family.

In conclusion, it has been shown that a direct (calibrationless) use of thermoporometry might be possible. Calibration performed for some linear alkanes yields a general law which relates the solvent freezing temperature inside a pore of diameter R_p to the normal freezing temperature, T_0 , of the solvent.

This law is very close to the one previously determined for substituted benzenes, and in particular, the a coefficient is the same (~ 1). These first results on two very distinct families of solvents tend to demonstrate a universal behavior of liquids confined in porous media.

References and Notes

- (1) Thomson, W. *Philos. Mag.* **1871**, 42, 448.
- (2) Brun, M.; Lallemand, A.; Quinson, J.-F.; Eyraud, C. *Thermochim. Acta* **1977**, 21, 59.
- (3) Liu, J.; Gan, L. M.; Chew, C. H.; Teo, W. K.; Gan, L. H. *Langmuir* **1997**, 13, 6421.
- (4) Kim, K. J.; Fane, A. C.; Ben Aim, R.; Lui, M. G.; Jonsson, G.; Tessaro, I. G.; Broek, A. P.; Bargeman, D. J. *J. Membr. Sci.* **1994**, 87, 35.
- (5) Neffati, R.; Apekis, L.; Rault, J. J. *J. Therm. Anal.* **1998**, 54, 741.
- (6) Luukkonen, P.; Maloney, T.; Rantanen, J.; Paulapuro, H.; Yliruusi, J. *Pharm. Res.* **2001**, 18 (11), 1562.
- (7) Jackson, C. L.; Mc Kenna, G. B. *J. Chem. Phys.* **1990**, 93, 9002.
- (8) Baba, M.; Nedelec, J. M.; Lacoste, J.; Gardette, J. L. *J. Non-Cryst. Solids* **2002**, 315, 228.
- (9) Wulff, M. *Thermochim. Acta* **2004**, 419, 291.
- (10) Takei, T.; Ooda, Y.; Fuji, M.; Watanabe, T.; Chikazawa, M. *Thermochim. Acta* **2000**, 352–353, 199.
- (11) Billamboz, N.; Baba, M.; Grivet, M.; Nedelec, J.-M. *J. Phys. Chem. B* **2004**, 108, 12032.
- (12) Landry, R. *Thermochim. Acta* **2005**, 433, 27.
- (13) Alnaimi, S. M.; Strange, J. H.; Smith, E. G. *Magn. Reson. Imaging* **1994**, 12, 257.
- (14) Baba, M.; Nedelec, J.-M.; Lacoste, J.; Gardette, J.-L.; Morel, M. *Polym. Degrad. Stab.* **2003**, 80, 2.
- (15) Billamboz, N.; Nedelec, J.-M.; Grivet, M.; Baba, M. *ChemPhysChem* **2005**, 6, 1–7.
- (16) Hench, L. L. *Sol-gel silica: processing, properties and technology transfer*; Noyes Publications: New York, 1998.
- (17) Baba, M.; Nedelec, J. M.; Lacoste, J. *J. Phys. Chem. B* **2003**, 107, 12884.